Accelerator Physics Research Topics at the Cornell Electron/positron Storage Ring

Abstract

The CESR operations group maintains an active research program covering a variety of topics with the purpose of maintaining and advancing its position the forefront of light source facilities, ensuring the continuing competitiveness of the Cornell High-Energy Synchrotron Source CHESS. Our work includes multiple submissions to each annual International Particle Accelerator Conference, as well as other venues, and is regularly published in refereed journals. This talk presents an overview of active areas of investigation.

Jim Crittenden

Accelerator Physics Seminar / Journal Club

3 November 2022

Table of Contents

Online dynamic aperture optimization techniques
See S.T.Wang journal club 10/13/2022

- Traditional method
  - Tuning iteratively (cycle through all variables manually or automatically)
- Robust conjugate direction search (RCDS) [1]
  - Powell's algorithm to minimize the objective and update the conjugate search direction
  - Robust line scan to find the minimum on each direction
  - Multi-variables but one objective (could expand to multi-objective)
  - Develop a conjugate direction set which cannot be modeled
  - Successfully demonstrated in several light sources (SPEAR3, ESRF, NSLS2, …)
- Dimension-reduction and genetic algorithm [2]
  - Reduce number of variables and create conjugate knobs
  - Demonstrated in the low emittance tuning (minimize vertical emittance) at CESR
- Machine-learning algorithm [3] and other algorithms

- Online DA optimization at CESR
  - Create conjugate DA knobs (Will Bergan, PhD thesis, 2020)
  - Tune with RCDS method

Relatively recently conceived project. Practical applications for CHESS ops.
Experiments scheduled for this February.
Stay tuned.

Transverse Resonance Island Buckets
See S.T.Wang journal club 10/13/2022

2nd stable orbit with Transverse Resonance Island Buckets - TRIBs

3rd order resonance
Island orbit closes
after 3 turns

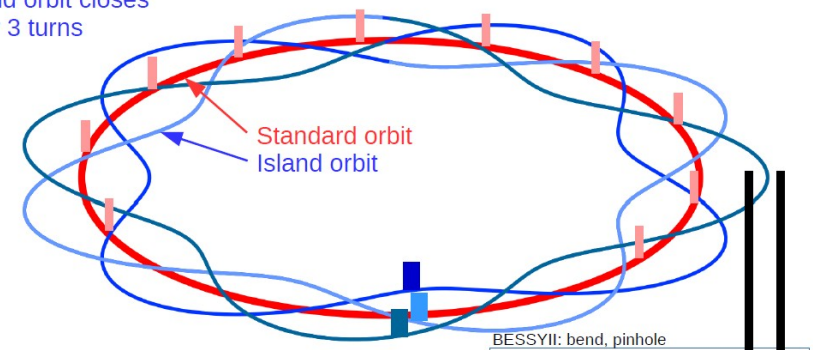

Two stable independent orbits capable to store **two independent fill pattern**

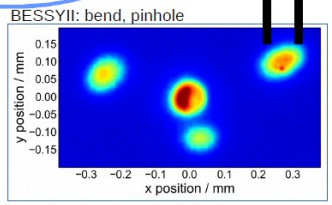

P. Goslawski, TRIBs at BESSY II

10th IPAC 2019, Melbourne, Australia

S.T.Wang and V. Khachatryan,Study of Transverse Resonance Island Buckets at CESR
IPAC'22, 14th International Particle Accelerator Conference,
MOPOST051,12-17 June 2022, Bangkok, Thailand

Tracking
1000 particles
@ 259.4 kHz

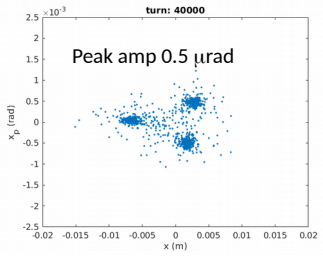

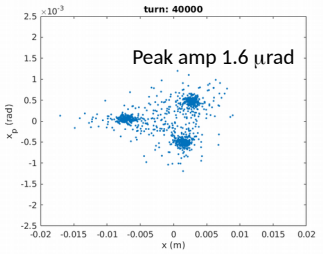

Apply island
clearing kick
(263 kHz, 0.674)

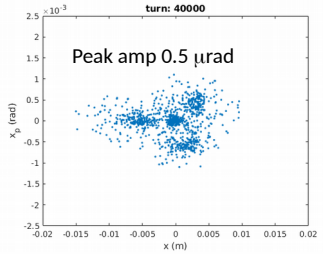

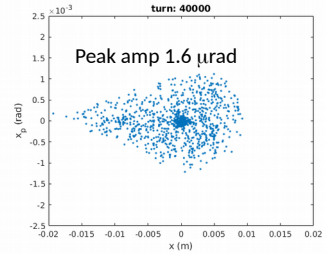

The single-shot image (one turn) from a gated camera shows the particles populate all three buckets.

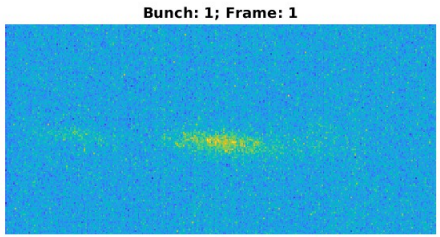

One turn

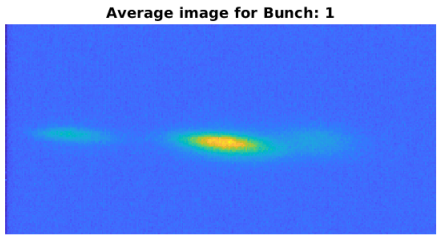

100 turn average

TRIBS demonstrated at CESR.

Successfully modeled using the Bmad software library, allowing validation of various effects such as the dependence on coupling.

Impedance measurements as a monitor of vacuum chamber history

Vacuum chamber heat damage discovered 10/25 by visual inspection during undulator installation.
Wall thickness: 0.5 mm. Aperture reduced from 4.6 mm to 2.3 mm.

1/14/22: eLog #1990

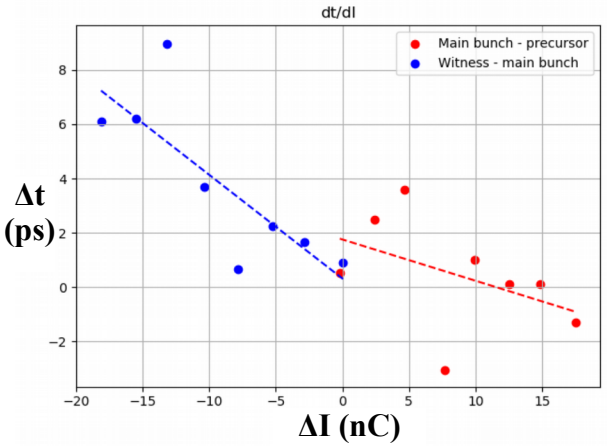

k_hom = -3.069 V/pC
w = 9.391 V/pC

10/25/22: eLog #2140

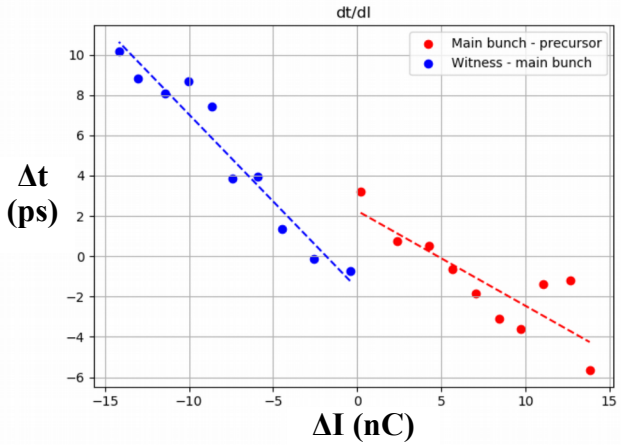

k_hom = -8.355 V/pC
w = 22.645 V/pC

Historical measurements of k_hom (2019-2022): -4.54 ± 1.04 V/pC

Tuesday's measurement is a significant increase in k_hom

Year-over-year monitoring of transverse and longitudinal impedance

This example shows the longitudinal impedance (higher order mode loss) measured using the arrival time difference of two bunches with differing populations.

This is a "smoking gun" showing a change likely due to a heating event.

Beam Position Detectors
Innovations in monitoring and diagnostics

The CESR Test Accelerator project (2004-2014) provided the CBPM system, which has turn-by-turn and bunch-by-bunch resolution.

Monitoring during CHESS operations

The leading bunch of the 45 bunches carries a fixed smaller bunch population (about 3e10 e-, 2 nC).
Its turn-averaged orbit is measured once per minute.

The beam current is topped off about every 10 minutes. During these injection cycles, turn-by-turn, bunch-by-bunch BPM data is recorded.

Ana Isabel Nica, 2021 REU program
Leveraging the Power of Neural Network AI to Improve the Precision on the Beam Position Reconstruction at CESR
Mentor: A.Chapelain

Project Examples

V. Khachatryan: Analysis of the turn-by-turn data with fits to noise, tunes, and orbit positions

A. Chapelain: Long-term database development and orbit history web pages

AC & STW: Detector signal distribution model parameterization to monitor pedestal width, time jitter and more

Next-generation BPM system at CESR

10 Hz continuous beam position monitoring:

✗ micron-level precision on x/y positions from averaging 1,000s of turns

✗ new hardware, firmware and software being designed and developed, e.g.: *full stack interactive web app for analyzing/monitoring current and past data*

- back-end (server side): databases storage for data and metadata, data processing and analysis and other behind-the-scene heavy lifting
- front-end (client side) : web-browser user interface to display and interact with monitoring information (analyzed data, data quality, alarms/warnings)

New interlock capability:

✗ BPM will provide interlock capability monitoring turn-by-turn x/y beam position → in-house custom made alternative to Libera BPMs that are currently used for beam position corrections and interlocking

CESR BPM errors

CESR BPM aims at sampling the top of the waveform from the 4 EM pick-ups. Sources of error thoroughly modeled in Monte Carlo simulations and compared to real data → sources well understood:

- ✗ sampling clock jitter σ_j
- ✗ peak alignment accuracy t_0
- ✗ signal to noise ratio σ_{snr}

} precision of ~10 microns on turn by turn position

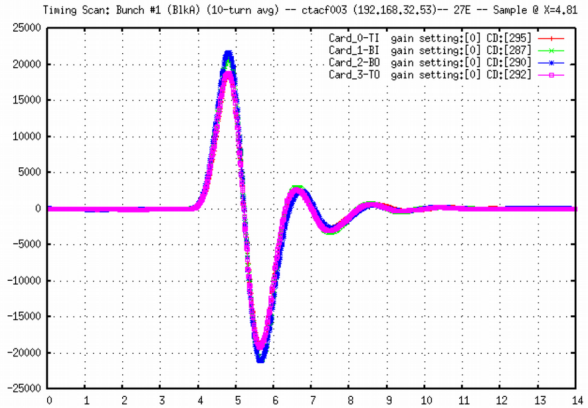

Developing method for *in-situ* error measurement using BPM data:

shape of readout distribution set by values of individual error sources → multiparameter fit. Fit uses our derived PDF for clock jitter and peak alignment:

$$f_X(x) = \frac{e^{-\frac{(acos(x)-\omega t_0)^2}{2(\omega\sigma_j)^2}} + e^{-\frac{(-acos(x)-\omega t_0)^2}{2(\omega\sigma_j)^2}}}{\omega\sigma_j\sqrt{2\pi(1-x^2)}}$$

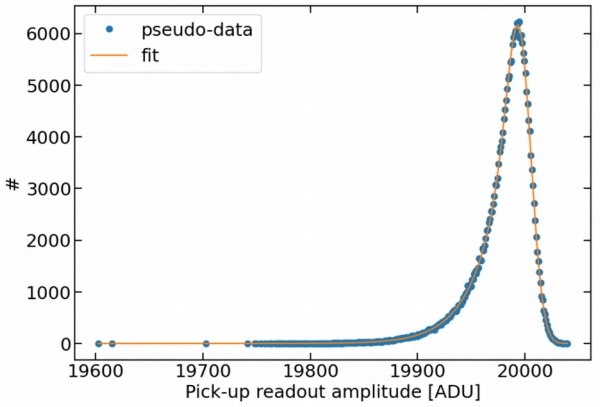

Analysis of bunch-by-bunch, turn-by-turn data
V.Khachatryan

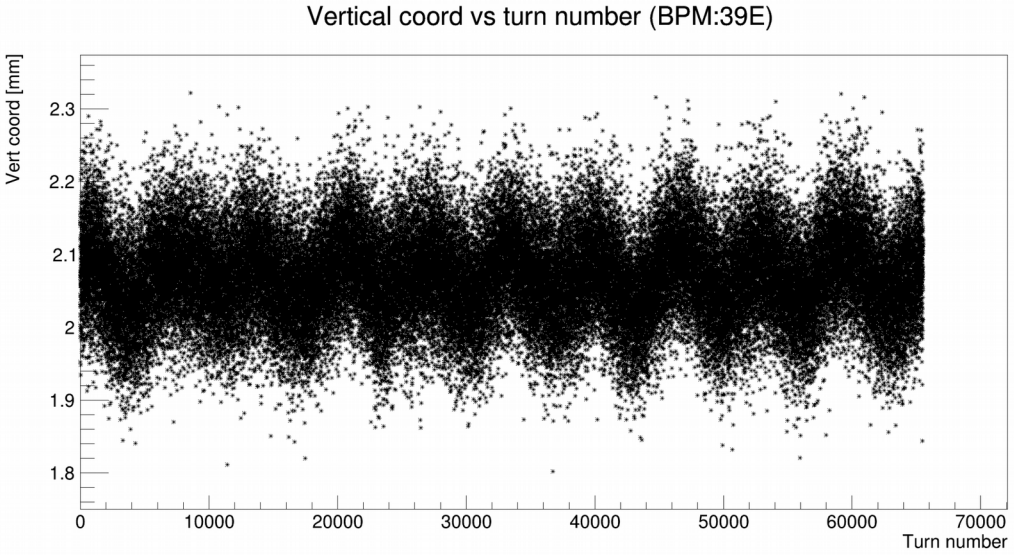

Phase and orbit analysis of t-b-t data

Noise analysis in reconstructed vertical orbit position oscillation.
Information available for all BPMs, so sensitive to ambient noise around the entire ring.

Fit to the vertical tune for subsets of turns including noise terms to identify sources of magnetic noise around the ring.

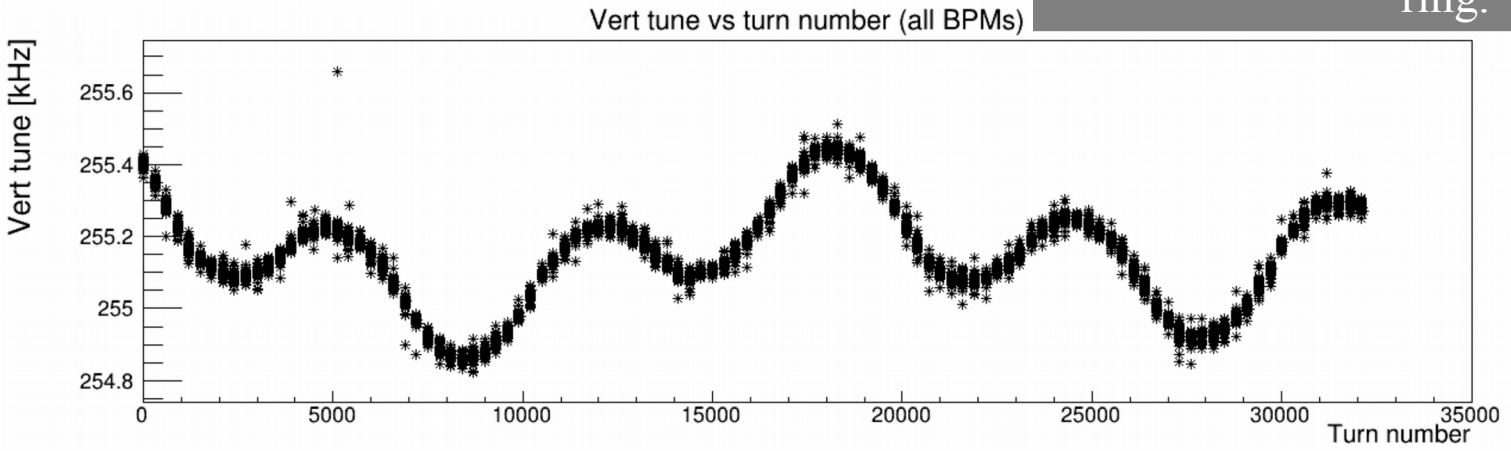

Ambient electrical noise: identification and mitigation

V.Khachatryan

V.K. et al, Magnetic Field Noise Search Using Turn-by-turn Data at CESR, *MOPOTK041, IPAC'22, Bangkok, Thailand*

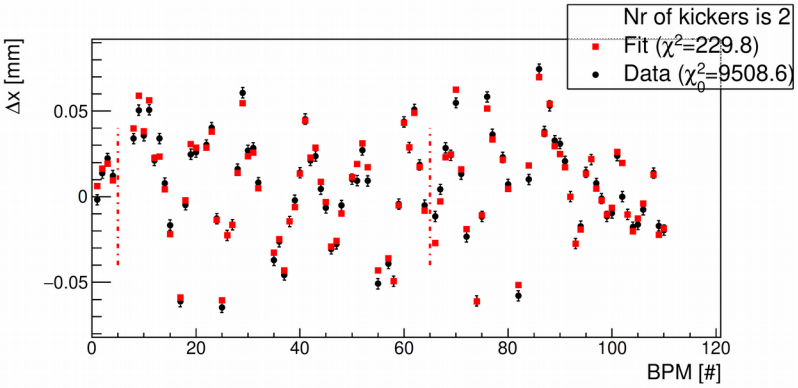

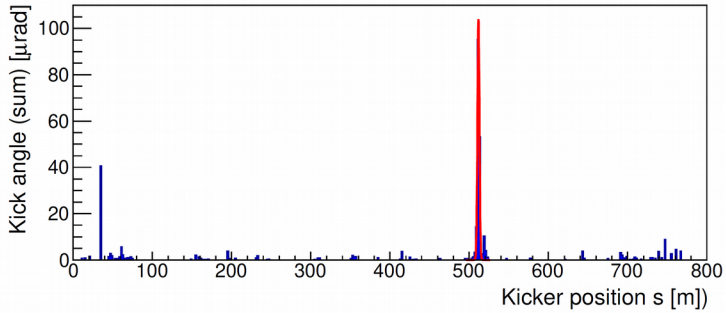

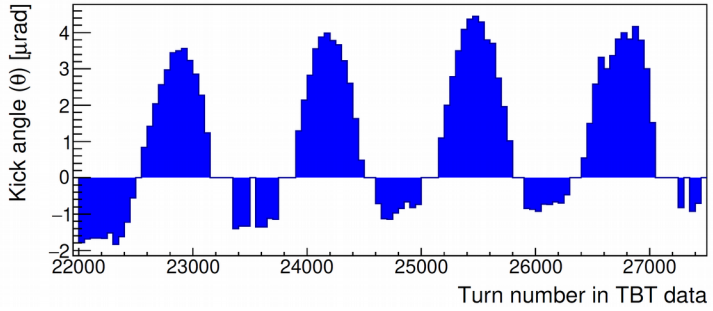

Noise source identification method: 300 Hz noise generated

- Induced 300 Hz noise at 510.2 m using a wave-form generator controlled magnet
- 65536-turn (2^{16}) data recorded
- The reference orbit is the average over all 65536 turns
- 50-turns are used for each orbit (difference) calculations.
- The analyzer found two kicks in this example: s_1=511.1 m, s_2=53.6 m, θ_1=3.5 μrad and θ_2=–0.57 μrad.

The summary plot for the sum kick angle (absolute) as a function of s-coordinate shows a sharp peak. The red curve is a Gaussian fit with mean at 511.6 m and σ=1.27 m.

The kick angle as a function of turn number shows the expected 300 Hz frequency (1300 turns between two peaks).

Analysis of t-b-t data identified locations of electrical noise. Sources found were fans, power supplies, and the synchrotron. Removing the sources reduced the noise in the data from 7.5μ to 3.5μ. Sensitivity to kicks was 1μrad (0.2 Gm) .

Systematics in the measurement of beam size using sextupole field strength scans

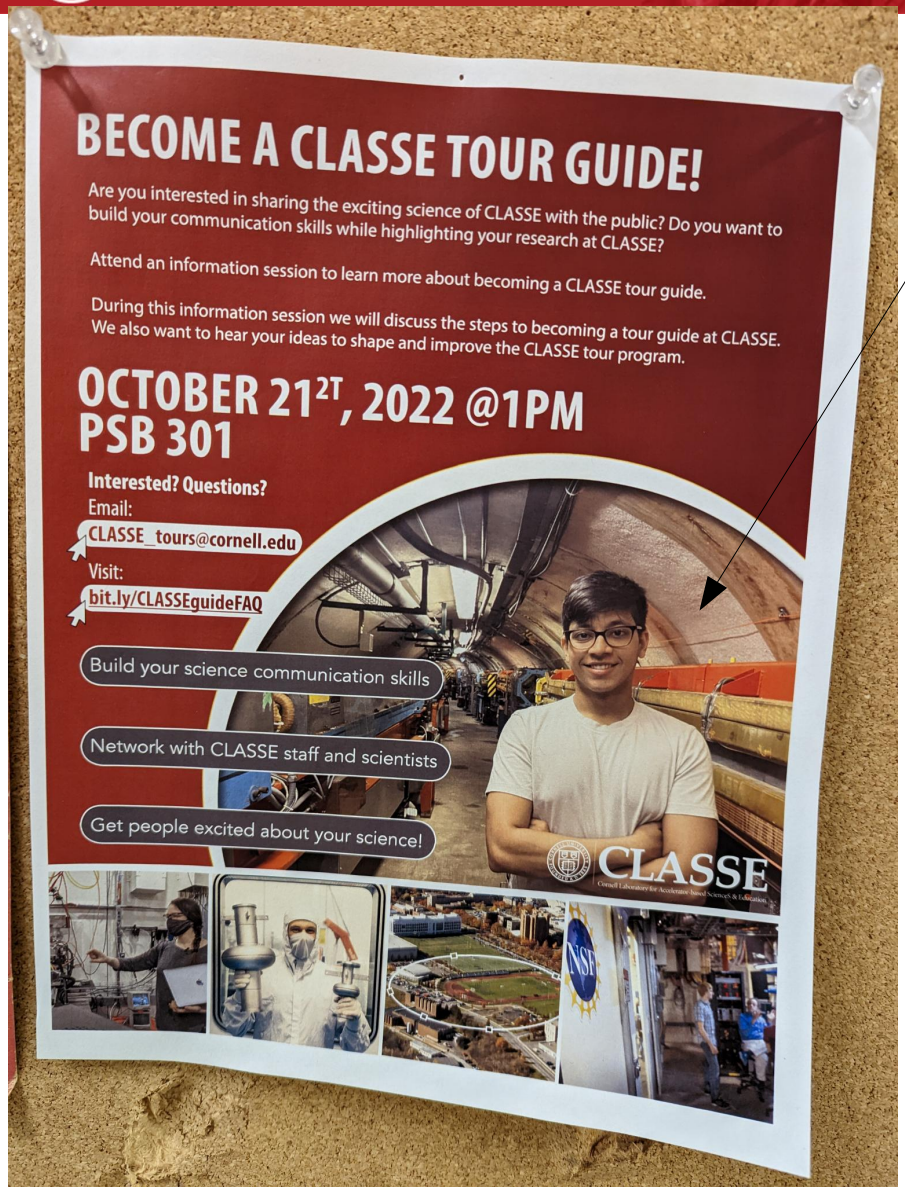

2022 CHESS-U REU Project
Ishaan Mishra
Rose-Hulman Institute of Technology
Mentors: J.C. and S.T.W.

Lorentz force equation

$$\vec{F} = q\,\vec{v} \times \vec{B}$$

Sextupole magnetic field

$$B_y(x) = B_0\,x^2$$

Beam bunch Gaussian charge distribution

$$q = q_0 \int_{-\infty}^{+\infty} \exp\left(\frac{(x - x_0)^2}{\sigma^2}\right) dx$$

Average force on the charge distribution

$$\langle F_x \rangle_{x_0,\sigma} = q_0\,c\,B_0 \int_{-\infty}^{+\infty} x^2 \exp\left(\frac{(x - x_0)^2}{\sigma^2}\right) dx$$

$$= q_0\,c\,B_0\,(x_0^2 + \sigma^2)$$

Measurement of beam size at the CESR sextupole magnets

Hannah Duan, Cornell undergrad research
Abigail Fagan, 2021 REU program
Ariel Shaked, Eng. Master's candidate 2023

J.C. et al, Measurement of Horizontal Beam Size Using Sextupole Magnets
IPAC'21, 13th International Particle Accelerator Conference, MOPAB253, May 2021, Campinas, Brazil (remote)

2D Analytic Derivation

Sextupole field components:

$$\frac{qL}{P_0}B_Y = \frac{1}{2}K_2L\,(x^2 - y^2) \qquad \frac{qL}{P_0}B_X = K_2L\,x\,y$$

Assuming initial $K_2L = 0$ and including parabolic and cubic terms, we have three equations with four unknowns:

$$\Delta K_1L = \Delta K_2L\,(X_0 + \Delta x) \tag{1}$$

$$\Delta p_Y = \Delta K_2L\,(X_0 + \Delta x)\,(Y_0 + \Delta y) \tag{2}$$

$$\Delta p_X = \frac{1}{2}\Delta K_2L\left[(Y_0 + \Delta y)^2 + \sigma_Y^2 - (X_0 + \Delta x)^2 - \sigma_X^2\right] \tag{3}$$

so,

$$2\,\Delta p_X = \Delta K_2L\left[\left(\frac{\Delta p_Y}{\Delta K_2L}\right)^2\left(\frac{\Delta K_1L}{\Delta K_2L}\right)^{-2} + \sigma_Y^2 - \left(\frac{\Delta K_1L}{\Delta K_2L}\right)^2 - \sigma_X^2\right]$$

which gives

$$\sigma_X^2 - \sigma_Y^2 = -2\,\frac{\Delta p_X}{\Delta K_2L} + \left(\frac{\Delta p_Y}{\Delta K_2L}\right)^2\left(\frac{\Delta K_1L}{\Delta K_2L}\right)^{-2} - \left(\frac{\Delta K_1L}{\Delta K_2L}\right)^2$$

Including only terms linear in ΔK_2L, we have

$$\sigma_X^2 - \sigma_Y^2 = -2\,\frac{\Delta p_X}{\Delta K_2L} + Y_0^2 - X_0^2.$$

Analysis of Difference Orbit and Phase Measurements

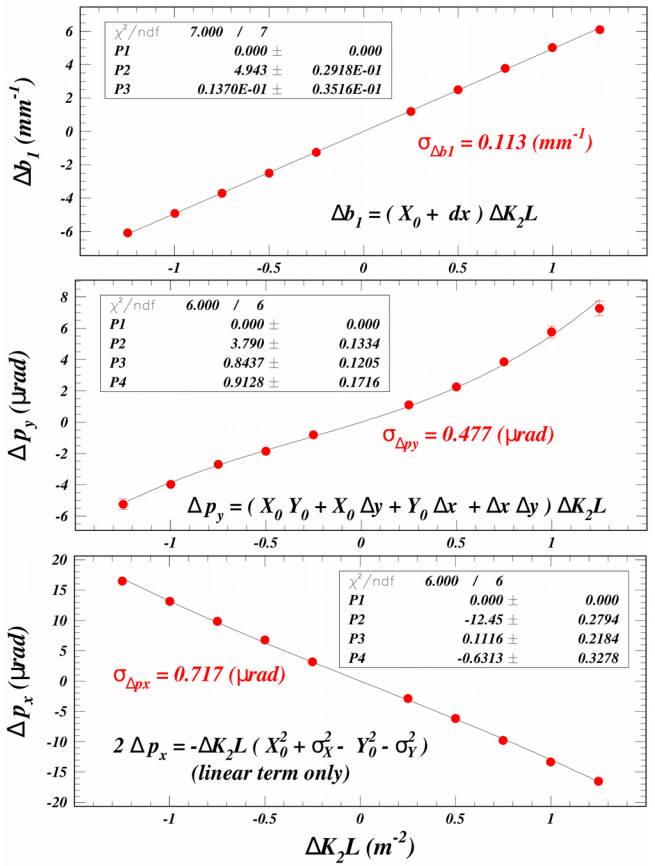

$X_0 = 4.943 \pm 0.029$ mm $X_0 Y_0 = 3.79 \pm 0.13$ mm^2 $Y_0 = 0.766 \pm 0.26$ mm $\Delta p_x/\Delta K_2L = -12.45 \pm 0.28\times10^{-6}$ rad/m^{-2} => $\sigma_x = 1.01 \pm 0.26$ mm

Beam-based alignment and calibration of the 76 CESR sextupole magnets

J.C. et al, *Progress on the Measurement of Beam Size Using Sextupole Magnets, MOPOTK040, IPAC'22, Bangkok, Thailand*

Example of tune change versus beam position strategy (D.Sagan / CesrV)

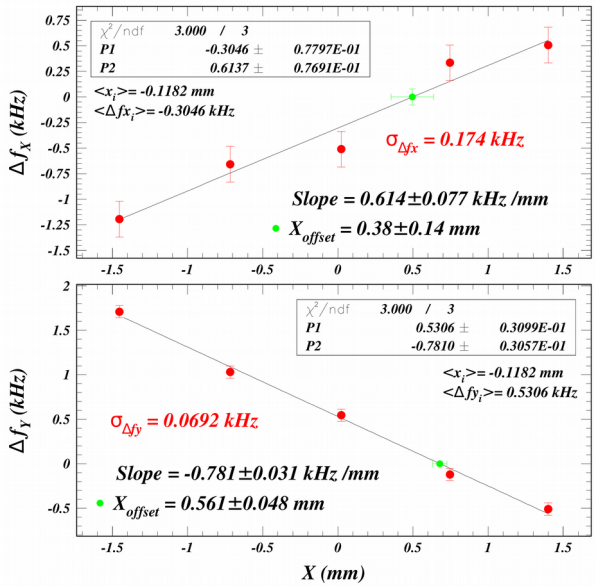

Calibration correction factor measurements and reproducibility for 76 sextupoles

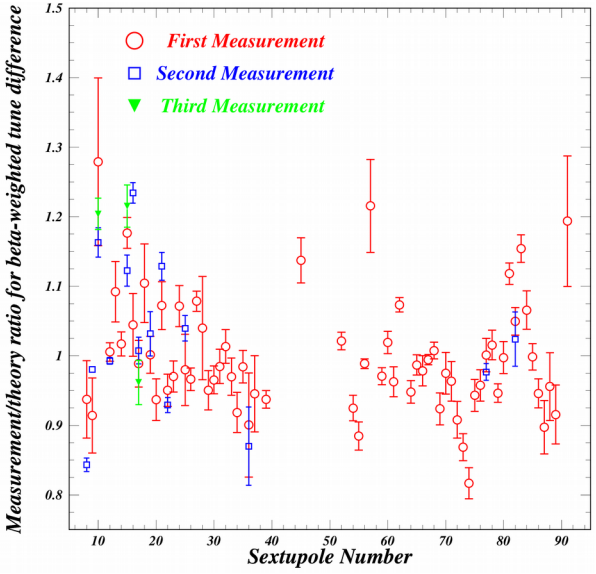

Sextupole offset measurements and reproducibility for 76 sextupoles

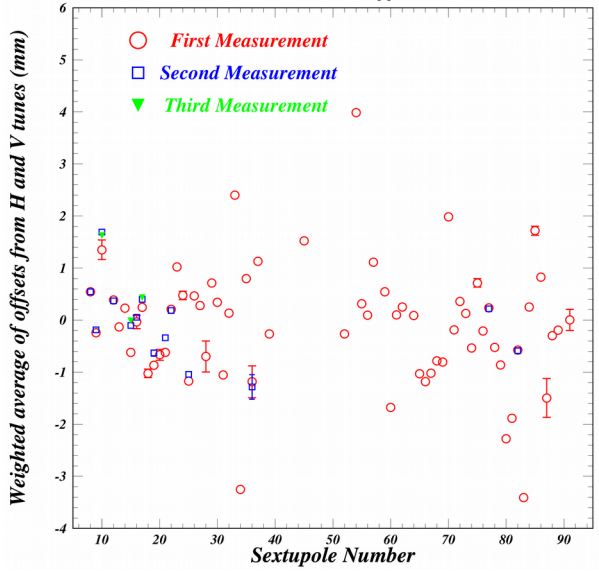

Our measurements of the calibration correction factors show an RMS deviation of 9.5% with a mean value of 1.009 ± 0.010. The uncertainties average 2.9% with an RMS spread of 2.0%.

With several exceptions, the RMS spread in the offsets is found to be 0.83 mm. The uncertainties average 43 microns with an RMS spread of 28 microns.

Ishaan's systematic error discovery
2022 REU project final report

Horizontal orbit kick slope determined from the difference orbit versus the sextupole offset assumed in the optics model

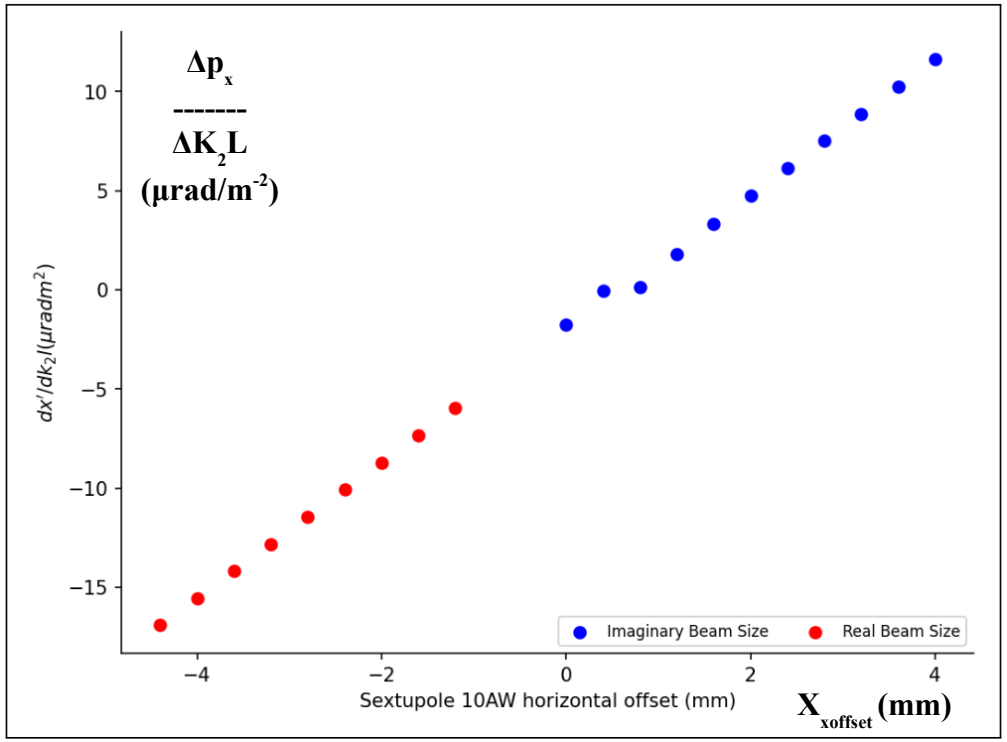

Figure 6: dx'/dk_2l plotted against the horizontal sextupole offset

There is a strong linear dependence on the value assumed in the lattice model for the sextupole offset in the result for the horizontal orbit kick slope $\Delta p_x/\Delta K_2 L$ obtained by fitting the difference orbit.

The analytic treatment above was based on the position of the beam relative to the center of the sextupole X_0. Now we will have to include the sextupole offset X_{offset}, with

$$X_0 = X_{orbit} - X_{offset}$$

The error in the beam size calculation will depend on the accuracy in our knowledge of the sextupole offset.

The sextupole offset can be obtained from the both calibration data and the κ_2 scan data. Investigations are underway.

Accelerator magnet design and analysis

J.C. & S.T.Wang, Comparison of Transfer Map Derivation Methods for Static Magnetic Fields,
IPAC'21, 13th International Particle Accelerator Conference, MOPAB253, May 2021, Campinas, Brazil (remote)

Nicole Verboncoeur, 2020 REU program

Half of one double achromat

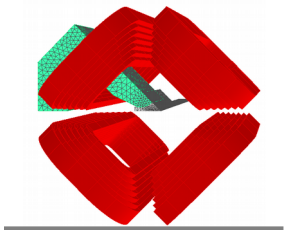

Finite-element model

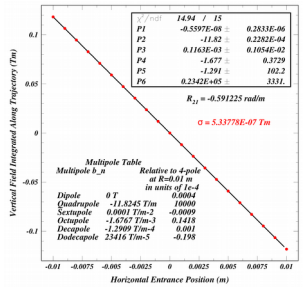

Analysis of the multipole content of the CHESS-U south arc quadrupole magnets comparing particle tracking results to the simple model implemented in the present CESR optics model used for design and operations.

J.C, Quantitative Assessment of Finite-element Models for Static Magnetic Field Calculations,,
Nucl.Instrum.Meth.A 1005 (2021) 165370

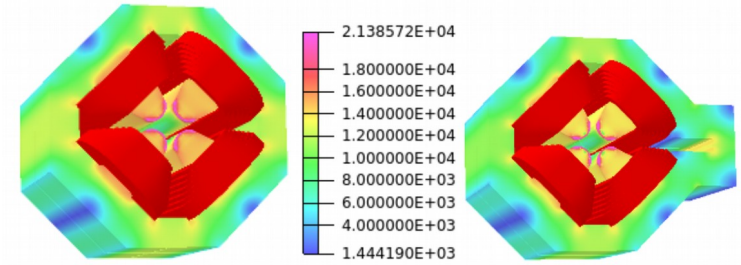

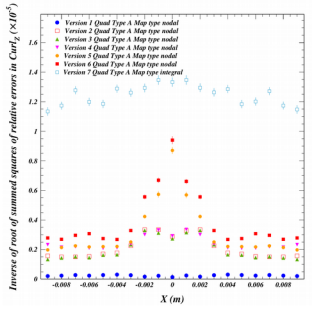

Two criteria:
1) numerical violations of Maxwell's equations,
2) "phantom multipoles" from numerical errors.

Also uses the example of the south arc quads.

Plots of accuracy as function of mesh refinement.

V. Khachatryan et al: Helical Wiggler Design for Optical Stochastic Cooling at CESR
IPAC'22, 14th International Particle Accelerator Conference, THPOPT066,12-17 June 2022, Bangkok, Thailand

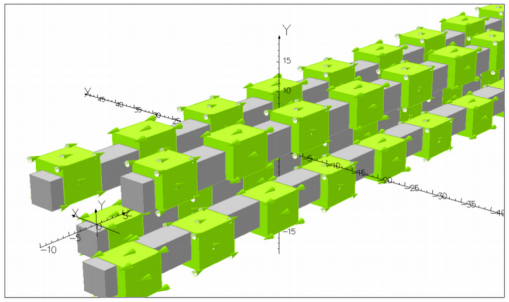

Helical wiggler magnet designed for field quality, power minimization and to protect against radiation damage.

Prototype built, field measured and compared to finite-element model.

Outstanding Machine Studies Topics

J. Shanks, Machine studies coordinator

- Beam stability development
  - L3/FOFB – VK
  - Position corrections
- CBPM gain calibration – ATC
- vBSM alignment – 2x4hrs – SW
- Sector 7 VBPM devel – Dobbins
- Radiation monitors – VK, JSh
  - Optimize gains
  - Calibrate
  - Benchmarking of new TLDs (RFL, JSh)
  - Sector 3 cave neutrons
- 200mA development
- 9x1 running – recover 100mA condx
- Impedance characterization – JSh
- TRIBs devel – 4x4hrs – SW
- Online DA optimization – 2x4hrs + 4x4hrs – SW

2022.10.27

The operations schedule includes one week of dedicated machine studies experiments in February 2023.

Submit MS Requests and shift requirements ASAP!

We wish to acknowledge generous support from the CHESS administration and Operations Director Mike Forster.

- Supplemental slides

HOML measurement technique
J.Shanks, MS meeting 27 Oct 2021

- Following M. Billing documentation (CBN 01-6)
- Loss factor k_{HOM} and wake W (as observed at one trailing bunch) are:

$$k_{HOM} = 2\pi f_{RF} < V > \sin\phi_{SR} \left(\frac{d\Delta t}{dq_{main}}\right) - \pi f_{RF} \left(\frac{R}{Q}\right) n_{cells} \exp\left[-\frac{1}{2}\left(\frac{2\pi f_{RF}\sigma_z}{c}\right)^2\right]$$

$$W = 2\pi f_{RF} < V > \sin\phi_{SR} \left(\frac{d\Delta t}{dq_{main}}\right) - k_{HOM}$$

→ Focus on k_{HOM} today

f_{RF} = RF frequency
<V> = Total RF voltage
ϕ_{SR} = Synchronous phase without beam loading
q_{main} = charge in main bunch (see next slide)
(R/Q) = property of RF cavities
n_{cells} = # of RF cavities
σ_z = bunch length

2021-10-27

CESR BPM errors

On a turn-by-turn basis, individual pick-up readout is expressed as:

$$\alpha_{amp} \times \beta_{gain} \times \gamma_{noise} \times cos\left[\omega(t_j + t_o)\right] + \delta_{pedestal}$$

- α_{amp}: waveform amplitude
- β_{gain}: readout gain: fixed
- γ_{noise}: electronics noise: tbt Gaussian random $g_Y(y)$
- t_j: clock jitter: tbt Gaussian random $f_x(x)$
- t_o: peak alignment: (fixed)
- $\delta_{pedestal}$: electronics pedestal: fixed

Many turns distribution can be obtained via the Mellin convolution of the PDFs:

$$h(y) = \int_{-1}^{1} f(x) g(\frac{y}{x}) \frac{dx}{x}$$

where PDFs are:

$$g_Y(y) = \frac{e^{-\frac{(y-y_0)^2}{2\sigma_{snr}{}^2}}}{\sigma_{snr}\sqrt{2\pi}} \qquad f_X(x) = \frac{e^{-\frac{(acos(x)-\omega t_0)^2}{2(\omega\sigma_j)^2}} + e^{-\frac{(-acos(x)-\omega t_0)^2}{2(\omega\sigma_j)^2}}}{\omega\sigma_j\sqrt{2\pi(1-x^2)}}$$

BPM signal amplitude distribution parameterization

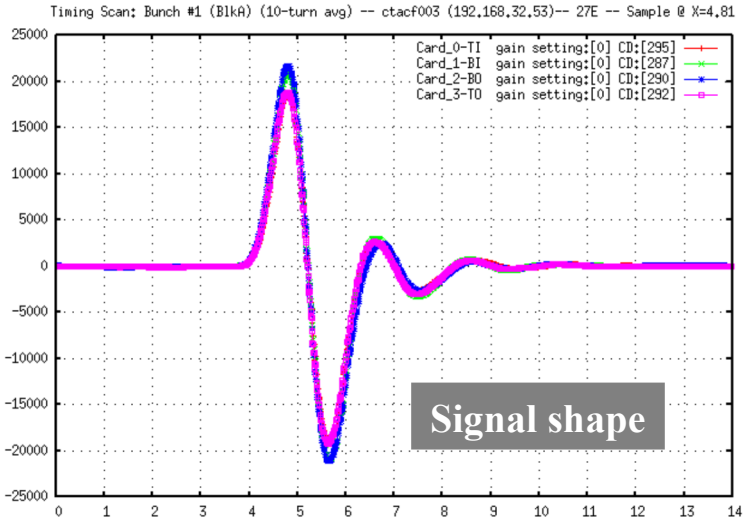

The probability density function for the pedestal jitter is Gaussian:

$$f(x) = \frac{e^{-\frac{(x-x_0)^2}{2\sigma_p^2}}}{\sqrt{2\pi}\sigma_p}$$

where x_0 is the average signal amplitude and σ_p is the pedestal jitter, which is typically ten counts out of a full range of 30k counts.
The probability density function for a time jitter σ_t (typically about 10 ps) and the timing error t_0 (typically a few ps) is

$$g(x) = \frac{e^{-\frac{(\arccos(x)-\omega t_0)^2}{2(\omega\sigma_t)^2}} + e^{-\frac{(-\arccos(x)-\omega t_0)^2}{2(\omega\sigma_t)^2}}}{\sqrt{2\pi(1-x^2)}\,\omega\sigma_t}$$

where $\omega = 2\pi f_{\text{filter}}$ and f_{filter} is the effective front-end filter frequency.
The probability density function for a product of density functions is given by the Mellin transform:

$$F(z) = \int_{-1}^{1} g(x) f\left(\frac{z}{x}\right) \frac{dx}{x}.$$